ELSEVIER

Biophysical Chemistry 69 (1997) 137–151

Biophysical Chemistry

Transient kinetics of substrate binding to Na^+/K^+-ATPase measured by fluorescence quenching

Promod R. Pratap [a,*], Edward H. Hellen [a], Anuradha Palit [a], Joseph D. Robinson [b]

[a] *Department of Physics and Astronomy, University of North Carolina at Greensboro, Greensboro, NC 27412, USA*
[b] *Department of Pharmacology, SUNY Health Science Center, Syracuse, NY 13210, USA*

Received 16 April 1997; accepted 2 June 1997

Abstract

This paper examines the transient kinetics of substrate binding to the Na^+/K^+-ATPase labelled with iodoacetamidofluorescein (IAF) using fluorescence quenching by trinitrophenyl–ATP (TNP–ATP). Earlier work (E.H. Hellen, P.R. Pratap, 1996, Fluorescence quenching of IAF–Na^+/K^+-ATPase via energy transfer to TNP-labelled nucleotide, Proceedings of the VIIIth International Conference on the Na^+/K^+-ATPase, in press) has shown that TNP-nucleotide binds to specific sites (from which unlabelled nucleotide *can* displace it) and nonspecific sites (from which unlabelled nucleotide *cannot* displace it). Under stopped-flow conditions, quenching of IAF-enzyme fluorescence was well described by a stretched exponential ($F(t) = F_\infty + \Delta F \exp[-Bt^\alpha]$). Physically, this function may be interpreted in terms of its inverse Laplace transform $\Phi(k)$, which describes a distribution of rate-constants; α reflects the width of this distribution. As TNP–ATP concentration increased, α decreased, reflecting TNP–ATP binding to sites with higher energy barriers. α decreased by about the same amount with increasing [TNP–ATP] in the presence of saturating ATP, indicating that the distribution of rate-constants is largely associated with the nonspecific binding sites. However, α was significantly less than 1 for ATP-induced fluorescence recovery in the presence of TNP–ATP, indicating that rate-constants associated with specific binding site are also distributed. The distribution of rate-constants for binding to the specific site indicates a distribution in the energy of the transition state for substrate binding. These results suggest that the specific binding site (in either the empty or the full state) may exist in a series of conformations separated by small energy barriers. However, the energy barriers for binding associated with these conformations are significantly distributed. © 1997 Elsevier Science B.V.

Keywords: Sodium pump; P-type ATPase; Reaction sequence; Conformational changes; Ion transport; Nonexponential kinetics

1. Introduction

The Na^+/K^+-ATPase uses the energy from the hydrolysis of ATP to move Na^+ and K^+ against their electrochemical gradients. A model for the reaction cycle for this enzyme was proposed by Albers and Post (see [1,2] for reviews) and elaborated by Karlish [3] where transport was coupled

Abbreviations: DMF, dimethylformamide; E_1 and E_2, two conformations of Na^+/K^+-ATPase; E_1P and E_2P, phosphorylated forms of E_1 and E_2; EtOH, ethanol; IAF, 5-iodoacetamidofluorescein; Na^+/K^+-ATPase, sodium plus potassium-dependent adenosine triphosphatase (EC3.6.1.3); TNP–ATP, trinitrophenyladenosine triphosphate; TNP–ADP, trinitrophenyladenosine diphosphate

* Corresponding author. Tel.: +1-910-334-5844; fax: +1-910-334-5865; e-mail: pratapp@dirac.uncg.edu

PII S0301-4622(97)00083-5

with ATP hydrolysis via a series of conformational changes. While ATP hydrolysis provides the energy for driving the overall reaction cycle, it is conceivable that partial reactions may be driven by energies of association and dissociation of various ligands. In this and previous papers [4–6], steady-state and stopped-flow kinetics of enzyme–nucleotide association were examined using the TNP-analog of the nucleotide.

Fluorescent probes have been used to examine various aspects of the enzyme reaction cycle. Several probes (such as IAF, FITC, RH421, and BIPM) have been used to examine conformational changes and charge transport by the enzyme [3,7–13]. Fluorescent probes have also been used to measure binding of various ligands to the enzyme: competition between eosin and ATP and the relaxation between free enzyme and enzyme associated with ATP or eosin has been used to determine rate-constants for ATP binding to the enzyme [14,15]; anthroylouabain has been used to examine cardiac glycoside binding to the enzyme [16].

Trinitrophenyladenosine triphosphate (TNP–ATP, a fluorescent analog of ATP that is not hydrolyzed by the Na^+/K^+-ATPase) has been used to examine the kinetics of nucleotide binding to the enzyme by measuring binding-induced fluorescence enhancement [17,18]. When the TNP analog of ATP or ADP binds to enzyme labelled with IAF, the fluorescein fluorescence is quenched [19]. This quenching, attributable to energy transfer between IAF and TNP, has been used to estimate the distances between IAF and the anthroylouabain binding site on the protein [19].

Quenching of IAF fluorescence by TNP-nucleotides can also be used as a signal of their binding to the enzyme. In earlier work, these quenching signals were used to distinguish between several models for substrate binding using TNP–ADP as a representative substrate [4–6]. In those experiments, the data could be best explained by a model where TNP–ADP bound the enzyme at two classes of sites: specific sites, which could bind either TNP–ADP or ADP, and nonspecific sites, which could bind only TNP–ADP. The affinity of TNP–ADP and ADP for the specific site was consistent with this site being the high-affinity ATP binding site involved in ATP hydrolysis resulting in ion transport. On the other hand, the nonspecific binding of TNP-nucleotide was nonsaturable over the concentration range examined (0–50 μM TNP–ADP in the presence of 15 nM enzyme). Preliminary analysis of IAF quenching by TNP–ATP gave similar results [6]. The data presented in this paper have been analyzed based on this result.

This paper examines the transient (stopped-flow) kinetics of TNP–ATP binding to the IAF-enzyme. In addition to being consistent with the results of the steady-state experiments, the results presented here suggest that the TNP–ATP binding exhibits fractal kinetics: i.e., binding sites evidently exist in a spectrum of conformations, each with slightly different internal energy, so that the rate-constants (and therefore, the energy barrier) for binding vary [20]. Ligand binding to enzymes has been analyzed in terms of fractals [21,22]. Other biological phenomena that exhibit fractal dynamics include the opening and closing of ion channels [23,24] and molecular relaxations [25].

2. Materials and methods

Frozen dog kidneys were obtained from Pel-Freez Biologicals (Rogers, AR). Na^+/K^+-ATPase was isolated from the outer medulla of the kidney by a modification of method C of Jørgensen [26]; specific activity was in the range of 10–25 μmol P_i (mg protein)$^{-1}$ min^{-1} at 37°C. Steady-state enzyme activity was measured either colorimetrically [27] or with a fluorescence assay [7,28] which couples the production of P_i to the conversion, by purine nucleotide phosphorylase, of the fluorescent substrate 7-methylguanosine to the nonfluorescent product, 7-methylguanine. Enzyme was labelled with IAF as described earlier [11,29].

Stopped-flow experiments were performed as described earlier [7,8] on a stopped-flow fluorimeter (Kinetic Instruments, Ann Arbor, MI) interfaced with a Macintosh IIcx personal computer (Apple Computer, Cupertino, CA) through a MacADIOS interface board (GW Instruments, Somerville, MA). Equal aliquots of enzyme (100 μg ml^{-1}) and TNP–ATP in identical buffers were rapidly mixed, and the fluorescence recorded from 1 ms to 4–32 s. Multiple shots

(typically 8–9) were averaged to yield mean fluorescence and standard error. The data from 2 ms to 4 s or 32 s were fitted by several (1–5) exponentials or with a 'stretched' exponential with or without an 'unstretched' exponential (see below) with a nonlinear least-squares fitting algorithm [30]. Fits yielded model parameters with estimates of standard errors.

2.1. Stretched exponentials

Chemical reactions kinetics exhibit stretched exponential kinetics if the rate-constants are time-dependent. Consider an irreversible first-order reaction:

$$T \rightarrow C \tag{1}$$

with a first-order rate-constants k_{TC}. Assume that k_{TC} is a function of time:

$$k_{TC}(t) = k_0 t^{\alpha - 1} \tag{2}$$

where $0 < \alpha \leq 1$. (Note that k_0 is in units of $s^{-\alpha}$ [31].) The usual chemical reaction would occur if $\alpha = 1$ (resulting in an 'unstretched' exponential). Eq. (2) implies that the rate-constant of the reaction decreases with time, i.e., the reaction slows down with time. Kinetic traces of these reactions are characterized by a rapid change at early times followed by slow changes at later times.

The concentration of T as a function of time is [31]

$$T(t) = T_0 \exp\left[-\frac{k_0 t^{\alpha}}{\alpha}\right] \tag{3}$$

For the experiments described here, T represents TNP–ATP concentration and C the complex it forms with the enzyme fragments. Note that the steady-state experiments have indicated that TNP–ATP binding does not saturate even at concentrations of 50 μM [5], indicating that the concentration of binding sites far exceeds the concentration of TNP–ATP. Further, the concentration of binding sites *does not* correspond to the enzyme concentration. Since the concentration of binding sites exceeds TNP–ATP concentration, binding may be treated as pseudofirst-order.

Once TNP–ATP binds, it quenches IAF fluorescence by fluorescence energy transfer. The total fluorescence of the sample will then be the sum of the quenched and unquenched IAF. It is assumed that IAF quenching is proportional to the concentration of the complex, C, in Eq. (1). The decrease in fluorescence will then be:

$$\Delta F = F_0 - F(t) = \phi[C](t)$$

where F_0 is the initial fluorescence, $F(t)$ is the fluorescence at time t after mixing, and ϕ is a proportionality constant related to the efficiency of energy transfer. This equation can be rewritten as:

$$F(t) = F_\infty + \Delta F \exp[-Bt^{\alpha}] \tag{4}$$

where F_∞ is the fluorescence intensity at infinite time (steady-state). ΔF is the magnitude of the fluorescence change, and $B = k_0/\alpha$; k_0 and α are defined in Eq. (3).

A similar result can be derived for a first-order reversible reaction, provided both forward and reverse rate-constants are assumed to have the same time-dependence.

The exponential term in Eq. (4) can be written as:

$$\exp[-Bt^{\alpha}] = \int_0^{\infty} \Phi(k) \cdot \exp[-kt]\,dk \tag{5}$$

That is, the stretched exponential can be written as a superposition of 'unstretched' exponentials. Here, $\Phi(k)$ is a distribution of rate-constants for these exponentials. Mathematically, $\Phi(k)$ is the inverse Laplace transform of the left-hand side term of Eq. (5). The stretch parameter α reflects the width of this distribution: if α is one, $\Phi(k)$ is a delta function; as α decreases, the distribution widens. Fig. 1 shows $\Phi(k)$ for representative values of α in the range found in this paper.

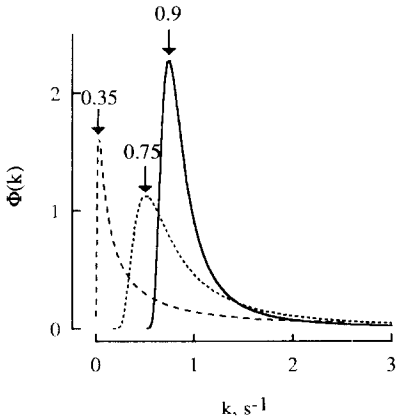

Fig. 1. Distribution of rate-constants at different α. The Laplace transform of a stretched exponential function ($\exp[-t^{\alpha}]$) was evaluated numerically at three different values of α.

3. Results

3.1. Kinetics of TNP–ATP binding

Fig. 2 shows typical quenching of IAF fluorescence with TNP–ATP: with an initial rapid decrease followed by a slow decrease, characteristic of stretched exponentials. Note that the time scale in Fig. 2 is logarithmic, to show clearly both the rapid and the slow changes on the same figure. These data were fitted with Eq. (4).

To compare this analysis with a more traditional approach, the data were analyzed with sums of exponentials. At a low TNP–ATP concentration (0.1 μM), the data could be fitted adequately to a single ('unstretched') exponential (as determined by the normalized chi-square). However, the number of exponentials required to provide an adequate fit increased as the amount of TNP–ATP was increased. For the example shown in Fig. 2, four 'unstretched' exponentials were needed to get a fit comparable (as determined by the normalized chi-squared) to that obtained with Eq. (4).

Table 1 gives the rate-constants and magnitudes (averaged over three experiments) for five exponentials fits to data with TNP–ATP concentrations from 0.5 to 15 μM. At lower concentrations, the magnitude of the fifth exponential was smaller than the root-mean-square difference between the data and the fit, so the corresponding rate-constant was omitted.

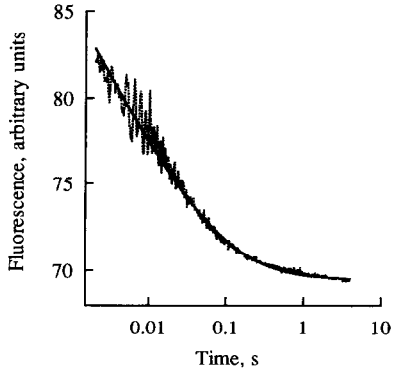

Fig. 2. Quenching of IAF fluorescence by TNP–ATP measured with stopped-flow fluorimeter. 100 μg ml^{-1} IAF enzyme in 150 mM choline chloride, 25 mM imidazole–HCl, pH 7, 1 mM EDTA, was rapidly mixed with 10 μM TNP–ATP in the same buffer (final concentration: 50 μg ml^{-1} enzyme, 5 μM TNP–ATP). The solid line is a fit to Eq. (4) (% $\Delta F = 33 \pm 1$, $B = 5.09 \pm 0.02$ s^{-1}, $\alpha = 0.269 \pm 0.005$).

Rate-constants for the first component (k_1) were large—these values represent components with half times less than or equal to 2 ms, the first time point analyzed. These components contributed significantly at early times, and these contributions were typically 1–2% ΔF.

The kinetics of IAF fluorescence quenching were examined as a function of TNP–ATP concentration. Data were fitted to Eq. (4). Only % ΔF (defined as $100 \cdot \Delta F/(F_\infty + \Delta F)$) and α varied significantly with [TNP–ATP] (Fig. 3). Values for B were typically between 5 and 10 s$^{-\alpha}$. The magnitude of fluorescence change (% ΔF) increased linearly with [TNP–ATP] over the concentration range examined here, and corresponded to the decrease in fluorescence observed under steady-state conditions at high TNP–ADP concentrations [4].

The 'stretch' parameter α decreased with TNP–ATP concentration. This parameter reflected the width of the distribution of rate-constants (and, therefore, energy barriers) for binding. Note that the fluorescence quench reflected the kinetics of those sites that are occupied by TNP–ATP. Therefore, at low [TNP–ATP], only the sites with relatively low energy barriers are occupied, resulting in a narrow distribution of rate-constants and a relatively high α. On the other hand, at high [TNP–ATP], sites with high energy barriers to binding will also be occupied, resulting in a wider distribution and a lower α.

Note that α at the lowest TNP–ATP concentration is significantly less than one (approximately 0.7). This appears inconsistent with the statement made earlier than these data (at 0.1 μM TNP–ATP) could be fitted to a single exponential (corresponding to an α of 1). In order to resolve this apparent contradiction, the data for 0.1 μM TNP–ATP and the fits to both a single exponential and a stretched exponential are shown in Fig. 4. The residuals for the fits are also shown.

When compared in terms of the normalized χ^2, both fits were equally good. However, the residuals (Fig. 4b) for the single exponential indicated the presence of an additional component. The fitting

Table 1
Variation of rate-constants with TNP–ATP concentration

[TNP–ATP] (μM)	Observed rate-constants (s^{-1}) (magnitude)				
	k_1 (% ΔF_1)	k_2 (% ΔF_2)	k_3 (% ΔF_3)	$10 \cdot k_4$ (% ΔF_4)	$100 \cdot k_5$ (% ΔF_5)
0.5	1030 ± 30 (6 ± 3)	27.3 ± 0.4 (2.4 ± 0.4)	4.20 ± 0.02 (4.3 ± 0.4)	4.8 ± 0.1 (1.0 ± 0.2)	–
1	390 ± 90 (1.2 ± 0.8)	35.4 ± 1.3 (3.8 ± 0.4)	5.55 ± 0.07 (5.9 ± 0.3)	5.4 ± 0.2 (1.2 ± 0.2)	–
2	1200 ± 40 (9 ± 3)	47.8 ± 1.0 (4.3 ± 1.5)	8.58 ± 0.04 (5.5 ± 0.3)	13.3 ± 0.6 (1.7 ± 0.2)	5.7 ± 0.3 (0.7 ± 0.2)
3	990 ± 40 (8 ± 2)	51.8 ± 0.8 (7.6 ± 0.2)	9.57 ± 0.07 (5.4 ± 0.2)	11.2 ± 0.1 (1.29 ± 0.13)	3.89 ± 0.04 (0.99 ± 0.12)
4	690 ± 30 (6.3 ± 0.8)	50.8 ± 0.9 (8.3 ± 0.5)	10.39 ± 0.08 (5.0 ± 0.8)	11.6 ± 0.4 (1.35 ± 0.07)	4.3 ± 0.1 (1.0 ± 0.2)
5	340 ± 70 (3.3 ± 1.0)	50.3 ± 1.0 (8.6 ± 1.0)	9.65 ± 0.07 (4.7 ± 1.1)	9.1 ± 0.2 (1.2 ± 0.2)	4.75 ± 0.05 (0.90 ± 0.09)
10	463 ± 6 (8.7 ± 0.7)	66.9 ± 0.7 (9.8 ± 0.4)	9.2 ± 0.3 (2.6 ± 0.3)	8.5 ± 0.2 (1.10 ± 0.11)	5.17 ± 0.07 (0.96 ± 0.08)
15	370 ± 9 (11.3 ± 0.8)	59.9 ± 1.1 (8.0 ± 0.6)	5.3 ± 0.2 (2.0 ± 0.2)	4.0 ± 0.1 (1.02 ± 0.10)	2.87 ± 0.07 (0.94 ± 0.06)

IAF enzyme in buffer (25 mM imidazole–HCl, pH 7, 150 mM choline–Cl, 1 mM EDTA) was rapidly mixed with varying amounts of TNP–ATP in the same buffer. The resulting fluorescence trace was fitted to a sum of five exponentials. The rate-constants and magnitudes (in parentheses) of these exponentials are shown here (average of three experiments ± standard deviation).

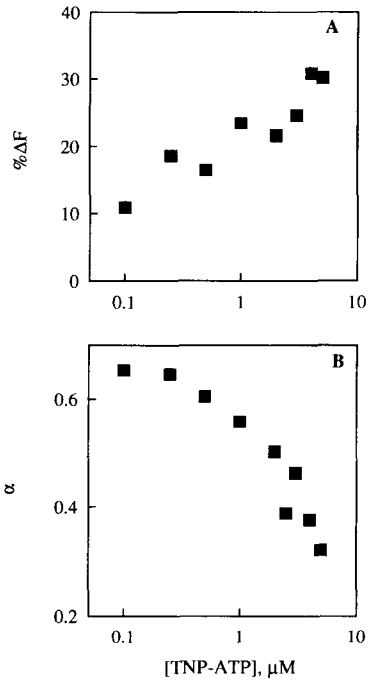

Fig. 3. (A) Magnitude (% ΔF) of fluorescence change as a function of TNP–ATP concentration. (B) α as a function of TNP–ATP concentration. Experimental conditions were the same as in Fig. 2, except, TNP–ATP concentration was varied as indicated.

algorithm could not resolve this component because its amplitude was too small.

3.2. Competition between TNP–ATP and ATP

Under steady-state conditions, when ATP was added to a preparation of enzyme + TNP–ATP, the fluorescence recovered, but not to the level before the addition of TNP–ATP [6,19]. In earlier work, fluorescence recovery was examined when enzyme + TNP–ADP was mixed with ADP. In those experiments, about 5% of the initial fluorescence could not be recovered when enzyme at nanomolar concentration with 1 μM TNP–ADP was mixed with saturating concentrations of ADP (4 mM) [5]. Extension of these results to TNP–ATP and ATP indicated that a certain fraction of the bound TNP–ATP could not be competed off with ATP, suggesting that TNP–ATP bound to two classes of sites: one, referred to as specific, could bind both TNP–ATP and ATP (and, hence, the TNP–ATP could be competed away by ATP); the other, referred to as nonspecific, bound only TNP–ATP.

To examine the differences in the transient-state binding of TNP–ATP to these different sites, two sets of experiments were performed. First, IAF-enzyme + 0.5 or 1 μM TNP–ATP was rapidly mixed with varying concentrations of ATP. The resultant fluorescence recovery reflected the displacement of TNP–ATP by ATP from the specific binding sites. Therefore, the kinetics of this fluorescence change reflect the binding of substrate to the specific binding sites. A typical fluorescence trace of this experiment is shown in Fig. 5.

Data were fitted either to a stretched exponentials (Fig. 5) or to a sum of two exponentials (not shown). Comparison of the normalized χ^2 for the two fits indicated that these fits were equally good. For fits to the stretched exponential, α ranged in value between 0.75 and 0.9 (Fig. 6), suggesting that the specific sites do not have as broad a distribution of rate-constants as seen with TNP–ATP alone (Fig. 3). In the double-exponential fit, the larger of the two rate-constants increased from 23.6 ± 1.2 to 135 ± 35 s^{-1} (a

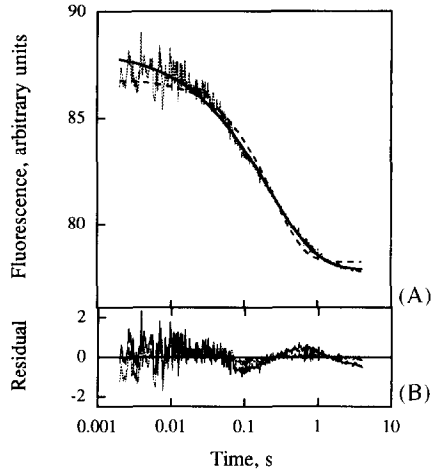

Fig. 4. (A) Fluorescence quenching of enzyme (100 μg ml^{-1}) rapidly mixed with 0.2 μM TNP–ATP (final concentration, 0.1 μM). Other experimental conditions as in Fig. 2. Dashed line: fit to a single exponential (% $\Delta F = 10.0\%$, $k = 4.05$ s^{-1}, root-normalized $\chi^2 = 0.602\%$). Solid line: fit to a stretched exponential (% $\Delta F = 11.8\%$, $B = 2.73$ $s^{-\alpha}$, root-normalized $\chi^2 = 0.492\%$). (B) Residuals: solid line, single exponential; dotted line, stretched exponential.

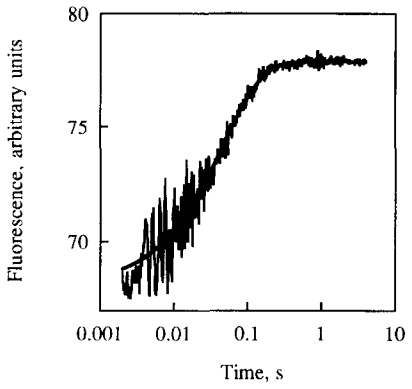

Fig. 5. ATP-induced fluorescence recovery. 100 μg ml^{-1} enzyme +0.5 μM TNP–ATP was rapidly mixed with 2 mM ATP. The solid line is a fit to Eq. (5) (% $\Delta F = \Delta F/(\Delta F + F_\infty) = 14.4 \pm 0.2\%$, $B = 11.7 \pm 0.5$ s^{-1}, $\alpha = 0.81 \pm 0.02$).

five-fold increase) when the ATP concentration increased from 250 μM to 2.5 μM.

In the second set of experiments, IAF-enzyme + 0.1 mM ATP was rapidly mixed with varying amounts of TNP–ATP. This concentration of ATP was much higher than the equilibrium constant for ATP binding to the enzyme [6,17]. The resultant quenching reflected the binding of TNP–ATP mainly to the nonspecific binding sites. Again, α as a function of [TNP–ATP] is shown in Fig. 7. The decrease in α under these conditions was similar to that seen in the absence of ATP (Fig. 3).

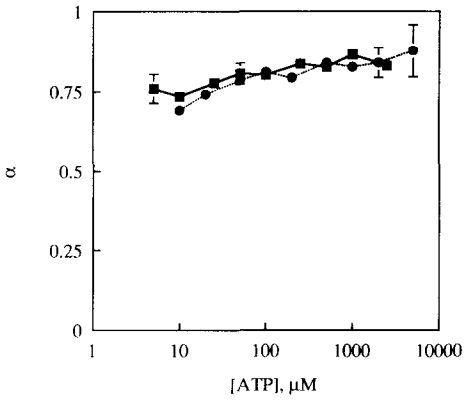

Fig. 6. α as a function of ATP concentration. Enzyme + 1 μM (filled squares) or 0.5 μM (filled circles) TNP–ATP was rapidly mixed with ATP. Other conditions were as in Fig. 2. Fluorescence increase was fitted with a stretched exponential.

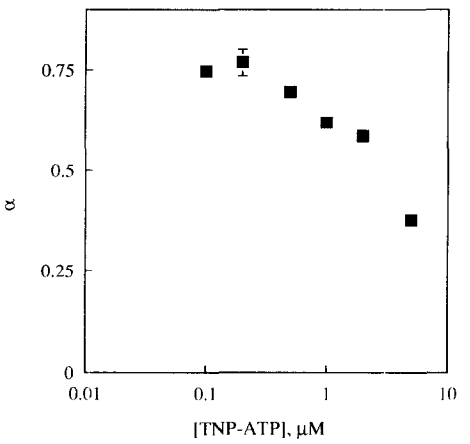

Fig. 7. α as a function of TNP–ATP concentration in the presence of 0.1 mM ATP. Other conditions same as in Fig. 2.

3.3. Inactivation controls

The variation in α indicates that a distribution of binding sites exists within the sample with varying

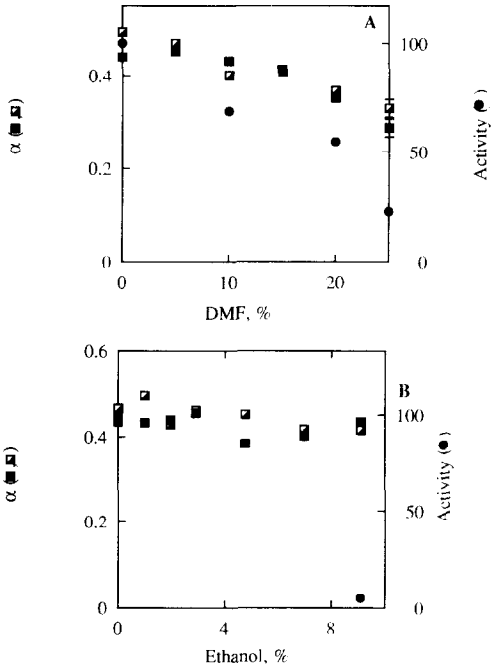

Fig. 8. Effect of DMF (A) and ethanol (B) on α and enzyme activity. Enzyme + ethanol or DMF (in ethanol) was rapidly mixed with 2 μM TNP–ATP + the same amount of EtOH or DMF. The filled and half-filled squares represent two different experiments. Activity was measured in parallel (filled circles). Activity in the absence of DMF and EtOH was defined as 100%.

energy barriers for binding. Either these variations are intrinsic to the protein or they are artifacts of the isolation and/or labelling procedures. To test for the latter, the enzyme was subjected to controlled inactivation, either with ethanol (EtOH) or with dimethylformamide (DMF), and quenching and enzyme activity were measured as functions of inactivator concentration. Fig. 8 shows α as a function of the amounts of EtOH and DMF, along with enzyme activity. With 9% ethanol (by volume), activity was reduced to 5% of maximum, while α was practically unchanged. Further increases in the amounts of EtOH did reduce α (data not shown). Increasing DMF to 25% (by volume) decreased activity to 23% of maximum, while α was reduced to 65% of maximum. Thus, while EtOH and DMF reduced both activity and α, the concentration dependence was different for these two inactivators.

4. Discussion

In this paper and the previous one [5], the quenching of IAF-enzyme fluorescence upon addition of TNP-nucleotide was used as a signal of TNP-nucleotide binding to the enzyme. Under steady-state conditions [5], it was shown that TNP-nucleotide binds to two classes of sites: specific sites (from which the TNP-nucleotide could be displaced by unlabelled nucleotide), and nonspecific sites (from which TNP-nucleotide could not be displaced by unlabelled nucleotide).

This paper examines the transient kinetics of IAF fluorescence quenching by TNP–ATP. These time-dependent fluorescence changes were nonexponential with time. In order to understand this nonexponential behavior, consider first the simplest possibility: that of the enzyme and TNP-nucleotide undergoing a simple association, with each enzyme molecule binding a single TNP-nucleotide molecule:

$$E + T \leftrightarrows C$$

where the enzyme (E) and TNP-nucleotide (T) combine to form a complex, C. (This model is considered here for completeness, even though steady-state kinetics have indicated the presence of specific and nonspecific binding sites.) The kinetics of this reaction is, in general, nonexponential; the enzyme fluorescence as a function of time is given by:

$$F(t) = F_\infty + \Delta F \frac{(1 - K) \cdot \exp(-k_{obs} t)}{1 - K \cdot \exp(-k_{obs} t)} \qquad (6)$$

where K and k_{obs} are functions of the forward and backward rate-constants and the initial concentrations of enzyme and TNP–ATP (E_0 and T_0). F_∞ is the fluorescence at infinite time, and ΔF is the change in fluorescence.

Two predictions can be made from Eq. (6). (a) It reduces to a single exponential either when $E_0 \gg T_0$ or when $T_0 \gg E_0$; i.e., if either reactant is in excess the reaction becomes pseudofirst-order; in other words, this model predicts exponential kinetics at low and high concentrations of TNP–ATP and nonexponential kinetics at intermediate concentrations. (b) At intermediate concentrations, Eq. (6) can be written as sum of exponentials (by expanding the term $1/[K - \exp(-k_{obs} t)]$ as an infinite series); the rate-constants of these exponentials are integer multiples of k_{obs}. Neither prediction is borne out experimentally; while the kinetics at low TNP–ATP concentration could be described by a single exponential, more and more exponentials were needed at higher concentrations of TNP–ATP; the rate-constants of exponentials are not multiples of the lowest value (Table 1).

An alternative model, still based on a single binding site can be proposed as follows: since the extent of quenching depends on the distance between TNP–ATP and IAF after binding, any changes in this distance after initial binding could result in nonexponential kinetics. These changes could be due to conformational changes that occur after binding. This process can be modelled as a cascade, with the initial step being complex formation. In order to simplify the calculation, and because multiple exponentials are apparent only at high TNP–ATP concentrations, the first step in this model is presented here under the approximation that $T_0 \gg E_0$, i.e., as pseudofirst-order. Consider, for example, a 2-step cascade:

$$E \leftrightarrows C \leftrightarrows C' \qquad (7)$$

Here, E is enzyme before binding, C is the initial complex which undergoes a conformational change to form C'. The first-order and pseudofirst-order rate-constants for this cascade are: k_1 for $E \rightarrow C$, k_2

for $C \rightarrow E$, k_3 for $C \rightarrow C'$, and k_4 for $C' \rightarrow C$. Note that k_1 is the product of the second-order rate-constant for TNP–ATP binding to the enzyme and the total [TNP–ATP] concentration.

Eq. (7) is governed by the differential equation:

$$\frac{d^2E}{dt} + \frac{dE}{dt}\sum_{i=1}^{4} k_i + E\sum_{i=1}^{2}\sum_{j=i+2}^{4} k_i k_j = k_1 k_4 E_0 \quad (8)$$

The solution to this differential equation is a sum of two exponentials:

$$E(t) = A_0 + A_1 \cdot \exp(-\lambda_1 t) + A_2 \cdot \exp(-\lambda_2 t)$$

where A_0, A_1 and A_2 are constants. The observed rate-constants for these exponentials are λ_1 and λ_2, which are solutions of the equation

$$\lambda^2 + \lambda\sum_{i=1}^{4} k_i + \sum_{i=1}^{2}\sum_{j=i+1}^{4} k_i k_j = 0 \quad (9)$$

To determine if λ has an extremum (maximum or minimum) with respect to the TNP–ATP concentration, it is enough to determine $\partial\lambda/\partial k_1$ and set it to zero. To determine this derivative, Eq. (9) is differentiated with respect to k_1 and then solved for $\partial\lambda/\partial k_1$:

$$\frac{\partial\lambda}{\partial k_1} = -\frac{\left(\lambda + \sum_{j=3}^{4} k_j\right)}{2\lambda + \sum_{j=1}^{4} k_j} \quad (10)$$

To determine the TNP–ATP concentration (or, equivalently, k_1) at which λ has an extremum, Eq. (10) is set to 0 and then solved for k_1. If $\partial\lambda/\partial k_1$ is zero, then

$$\lambda + \sum_{j=3}^{4} k_j = 0 \quad (11)$$

λ is the root of a quadratic equation, and is given by:

$$\lambda = \frac{-\left(\sum_{i=1}^{4} k_i\right) \pm \sqrt{\left(\sum_{i=1}^{4} k_i\right)^2 - 4\sum_{i=1}^{2}\sum_{j=i+2}^{4} k_i k_j}}{2} \quad (12)$$

By substituting λ from this equation into Eq. (11), a relationship involving the four rate-constants is obtained:

$$(k_1 + k_2 - k_3 - k_4)^2 = (k_1 + k_2 + k_3 + k_4)^2 - 4[k_1(k_3 + k_4) + k_2 k_4] \quad (13)$$

This relationship is valid only if the product $k_2 k_3 = 0$, that is, if the initial binding step is irreversible. Under those conditions, Eq. (13) is an identity and is true for all k_1: there is no concentration of TNP–ATP where the observed rate-constants are at an extremum. Thus, the cascade model predicts that λ must change monotonically with [TNP–ATP]. This argument may be generalized to cascades with more than two steps.

This prediction (of monotonically changing k_{obs}) is not consistent with the parameters obtained from the data: Table 1 gives the results of fits of fluorescence traces to 5 exponentials as a function of TNP–ATP concentration: k_2, k_3 and k_4 increase with [TNP–ATP] at low concentrations but decrease at higher concentrations, while k_5 decreases at low and then increases at high concentrations.

The parameters shown in Table 1 were obtained from fitting data from 2 ms to 32 s. The first four rate-constants (k_1 through k_4) were not significantly different when the fits were restricted to the first four seconds (in order to compare with the stretched exponential fits shown in Fig. 2). Note that several of the values obtained for k_1 are unrealistic for data over this range in time: an exponential with an observed rate-constant of 1000 s^{-1} has a $t_{0.5}$ of 0.7 ms, and its amplitude is only 14% of its maximum at 2 ms, the first time point of the analyzed data. This component accounted for some of the features at early times, and because of its small size, will not be discussed further. The arguments presented here against the simple binding model were made using the parameters k_2, k_3, and k_4.

These problems with simple binding models suggest that the quenching kinetics are intrinsically non-exponential. Such kinetics typically describe reactions that occur in inhomogeneous media, for example, reactions that occur at surfaces or in amorphous media such as glasses [31]. These kinetics have been described successfully with stretched exponentials. Since the binding of TNP–ATP to the Na^+/K^+-ATPase occurs at a surface (that of membrane fragments), this description appears to be appropriate.

Further, steady-state kinetics suggest that TNP-nucleotide binds to heterogeneous sites on the membrane [4–6]. The time-course of TNP–ATP binding exhibits properties characteristic of stretched exponentials: an initial rapid decrease in fluorescence followed by a slower decrease (Fig. 2).

4.1. Physical interpretation of stretched exponentials

As mentioned earlier, the kinetics of IAF fluorescence quenching cannot be explained in terms of sums of exponentials, but could be fitted with a single 'stretched' exponential (Eq. (6)). This section proposes a possible physical interpretation of these kinetics

Mathematically, any decaying function $f(t)$ can be expressed as a Laplace transform, i.e., as a superposition of an infinite number of exponentials (limited only by requirements of continuity and boundedness). The stretched exponential can be expressed in this fashion, as shown in Eq. (5).

Physically, Eq. (5) can be interpreted in the following manner: consider the population of binding sites in the sample when TNP–ATP is mixed with the enzyme. Steady-state experiments have already indicated that these binding sites are heterogeneous, with specific and nonspecific sites (where ATP can and cannot affect TNP–ATP binding, respectively [5,6]). In all likelihood, TNP–ATP binds to different sites with different rate-constants, with these rate-constants distributed in some fashion.

In Eq. (5), each exponential on the right represents a reaction with a different energy barrier for binding. The coefficient of the exponentials ($\Phi(k)$) represents a distribution of rate-constants, and therefore, a distribution of activation energies; in other words, $\Phi(k)$ is an indication of the fraction of sites that are characterized by the observed rate-constant k. Fig. 1 shows this distribution function for various values of the parameter α. These distributions were determined as follows: data were fitted by the stretched exponential function (Eq. (4)), yielding estimates for k_0 and α; then, the inverse Laplace transform $\Phi(k)$ was then evaluated numerically. Any function $f(t)$ which fits the data as well as the stretched exponential will give the same $\Phi(k)$. In that sense, the stretched exponential is a *parametrization* of the data.

Thus, the distribution $\Phi(k)$ is the physically significant quantity here, and may be interpreted in terms of a distribution of binding sites with different activation energies [20]. Note that in the experiments shown in Figs. 2 and 3, no distinction was made between the specific and nonspecific sites. This distribution of activation energies may indicate that the binding sites may exist as a distribution of conformations, each conformation separated from others by relatively small energy barriers; it may also indicate different environments for the different binding sites.

This interpretation can also account for the broadening of the distribution with TNP–ATP concentration: at low concentrations, only the sites with the lowest activation energies are filled. As TNP–ATP concentration increases, sites with higher activation energies are filled, resulting in the observed broadening of $\Phi(k)$.

4.2. Binding of TNP–ATP and ATP to specific sites

Steady-state measurements indicated that TNP-nucleotide bound to specific and nonspecific binding sites [4,5]. Specific sites were those where ATP could affect TNP–ATP binding (by displacing it), while nonspecific sites were those where ATP could not affect TNP–ATP binding. Those experiments yielded equilibrium constants for the specific binding sites for nucleotide and their TNP-analogs.

In this paper, the kinetics of substrate binding to the specific sites were examined by rapidly mixing ATP to a mixture of enzyme and TNP–ATP (Fig. 5). The resultant fluorescence recovery reflected the displacement of TNP–ATP by ATP from the specific binding sites. Since the ATP concentrations used here were much higher than the dissociation constant for ATP (0.1 μM [6]), these kinetics represent TNP–ATP dissociation from these sites. These kinetics could be fitted well either with a sum of two exponentials (fits not shown) or with a stretched exponential with an α of 0.8–0.9, indicating that the specific binding sites also exist as a distribution of conformations. However, this distribution is not as wide as that for the nonspecific sites (Fig. 7).

It may be argued that the fit to a sum of two exponentials is physically simpler and easier to interpret than the stretched exponentials. Since the fluorescence recovery is determined by the rate of TNP–

ATP dissociation, this model predicts that when 0.5 μM TNP–ATP + enzyme is rapidly mixed with 0.25–2.5 mM ATP, the observed rate-constants must be independent of ATP concentration. This prediction was not borne out in the experiments: the larger of the two rate-constants varied strongly with ATP concentration over the entire range of concentrations used (a 5-fold increase in rate-constant corresponding to a 10-fold increase in ATP concentration). These results indicated that the two-exponential model could not explain the data.

A similar argument regarding the dependence of parameters on ATP concentration may be made about the stretched exponential fit. Of all the parameters obtained from these fits, only B varied marginally with ATP. In two experiments, B increased, varied from 12.3 to 12.8 and 11.8 to 16.0 when [ATP] increased from 250 μM to 2.5 mM. This change is much smaller than the changes observed in the rate-constants in the two-exponential fit.

Note that steady-state experiments indicated a definite equilibrium constant for TNP–ATP (and ATP) binding to the specific site [5,6]. Thus, although the ratio of the forward and backward rate-constants was a constant (i.e., time-independent), the individual rate-constants depended on time (as described in Eq. (2)). The two rate-constants must, therefore, have the same time-dependence.

As discussed earlier, the time-dependence of the rate-constants (and the stretched exponential kinetics derived from it) reflect a distribution of activation energies. Here, each rate-constant for binding to the specific site is considered separately. The forward rate-constant reflects the energy differences between the initial, unbound state and the transient activated state. The distribution of rate-constants may be the result of a distribution of the free energies of the unbound state, the transition state, or both. However, since there exists a definite equilibrium constant for substrate binding to the specific sites, it is unlikely that the energies of the unbound states are distributed to any extent. (The width of this distribution must be smaller than the thermal energy.) Thus, a possible explanation of the distribution of rate-constants may be a distribution of the energies of the transition states. A similar argument can be made for the backward rate-constants. In other words, the distribution of rate-constants and the existence of a definite equilibrium constant implies that the energy of the transition state is distributed (Fig. 9), while the energies of the initial (unbound) and final (bound) states are not.

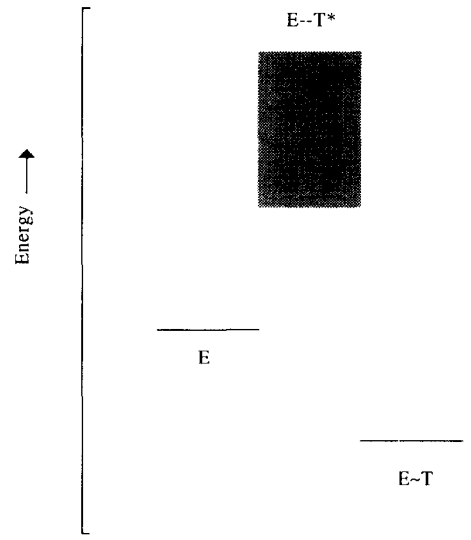

Fig. 9. Schematic representation of energy levels of different forms of the enzyme: E = binding site occupied; $E \sim T$ = binding site occupied; $E-T^*$ = transition state. The transition state is shown as a shaded box to denote the distribution of energies in this state. See text for discussion.

4.3. Nonspecific binding sites

In order to probe nonspecific binding sites, IAF fluorescence quenching by TNP–ATP was measured at high ATP concentration: since ATP blocks TNP–ATP binding to the specific sites, these experiments would only probe the nonspecific sites.

These experiments indicated that the variation in barriers seen when IAF fluorescence was quenched with TNP–ATP in the absence of ATP was mainly due to the nonspecific binding sites. Both in the absence (Fig. 3B) and presence (Fig. 7) of ATP, α decreased with increasing TNP–ATP concentration over practically the same range. A significant difference was seen at higher TNP–ATP concentration between α in the absence (Fig. 3B) and presence (Fig. 7) of ATP: in the absence of ATP, α decreased more than in the presence of ATP. This difference could be attributable to TNP–ATP binding to the specific sites in the absence of ATP.

In the case of binding to the specific sites, comparison between steady-state and transient state kinetics yielded the conclusion that the distribution of rate-constants was due to a distribution of the energy of the transition state and not to a distribution of the unbound or bound states. A similar conclusion cannot be made for nonspecific binding, because a definite equilibrium constant for this binding could not be determined [5].

4.4. Other considerations

Structural studies of the α subunit of the enzyme have indicated that about 50% of the amino acids are located in a cytoplasmic loop between the fourth and fifth transmembrane domains [1]. The ATP and IAF binding sites are located on this loop. Very little is known about the higher-order structure of this loop. Preliminary results have indicated that a peptide containing the ATP binding site overexpressed in *E. coli* retains the ability to bind ATP [32]. This result implies that the ATP binding properties of the enzyme depend largely on the structure of the cytoplasmic loop.

Although the Na^+/K^+-ATPase is a transmembrane protein, the cytoplasmic loop can be thought of as a globular protein anchored to the membrane. Stretched exponentials have been used to examine the dynamics of globular proteins ([20] and references therein), and those studies may be used to interpret results reported in this paper. Experiments on globular proteins (such as myoglobin) suggest that they have potential energy functions with a large number of shallow minima [33], consistent with a distribution of rate-constants. Further, molecular dynamic simulation of myoglobin based on its static crystallographic structure indicated that oxygen could not reach its binding site because of a large energy barrier. However, small perturbations in the structure (not apparent from crystallographic analysis) could allow oxygen to enter into the binding pocket [33]. These fluctuations may be akin to the distribution of conformations suggested here, and may account for the distribution of rate-constants seen for specific binding (as reflected by $\alpha < 1$; Fig. 6).

Questions remain about the nature and location of the nonspecific binding sites. In analyzing their data, Moczydlowski and Fortes [17] assumed that TNP–ATP binds to a single site; in their subsequent analysis, they found that TNP–ATP binds to this site with greater affinity than ATP. It was conjectured that the trinitrophenyl group inserts into hydrophobic regions in the protein to stabilize binding. Although data presented here and earlier [5] could not be fitted with a single-site model, the hydrophobic nature of the trinitrophenyl group may explain the nonspecific binding: because of this group, TNP–ATP may bind to sites in the planar lipid bilayer and/or within the protein itself, sites that are unrelated to the ATP binding site. The energy barrier for this binding would then vary, depending on the environment at these sites. Further, there may be a large number of such sites per protein molecule.

A final question needs to be addressed: if rate-constants for binding were time-dependent (Eq. (2)), why did this time-dependence not appear in earlier experiments that examined later steps in the reaction cycle [7–9]? In other words, why did the kinetics of charge transfer and of conformational changes associated with ion transport fit well to one exponential?

There are two possible explanations. The first is that with the enzyme preparation and labelling protocol used here, only 30–50% of the enzyme was active. It is possible that a fraction of the inactive enzyme bound substrate, (and, thus, contribute to the binding signal), but could not transport. The distribution of rate-constants may be due to these inactive enzyme molecules.

An attempt was made to address this question using controlled inactivation of the enzyme with ethanol and DMF. These experiments did not yield definitive conclusions: while controlled inactivation with ethanol destroyed activity without changing α, inactivation with DMF did reduce α (although not to the extent of reduction in activity). It is possible, indeed likely, that the mechanisms of enzyme inactivation in these experiments are different from enzyme inactivation during preparation.

The effect of varying levels of activity was examined under steady-state conditions [5]. In those experiments, data analysis yielded an 'active fraction' parameter that represented the fraction of the enzyme that bound TNP-nucleotide to the specific binding site. This parameter correlated well with enzyme activity: a two-fold increase in the active fraction

reflected a two-fold increase in enzyme activity. These experiments indicated, therefore, that enzyme rendered inactive during preparation did not bind TNP-nucleotide at the specific site. Further questions about the effects of enzyme activity levels will be addressed in the future by examining substrate binding to different enzyme preparations made with protocols that yield higher fractions of active (or inactive) enzyme.

An alternative explanation involves the magnitudes of binding rates. Earlier, it was argued that the observed rate-constant in the ATP-induced fluorescence recovery experiments reflected the rate-constant of TNP–ATP dissociation from the specific binding site. It was also argued that because of the time-independence of the dissociation constant for TNP–ATP from this site, the time-dependence of the forward and reverse rate-constant for TNP–ATP at this site must be the same. The time-dependent dissociation (reverse) rate-constant for TNP–ATP is given by Eq. (14):

$$k_2(t) = k_{20} t^{\alpha - 1} \tag{14}$$

Typical parameters are: $\alpha = 0.81$, and $k_{20} = 10\ s^{-\alpha}$ (from Fig. 5; $B = k_0/\alpha$).

The dissociation constant ($K_d = k_2/k_1 = k_{20}/k_{10}$) for TNP–ATP is of the order of 10^{-7} M [6]. Therefore, $k_{10} = 10^8\ M^{-1}\ s^{-\alpha}$. Using these parameters and Eq. (2), k_1 and k_2 can be calculated at 2 ms and 4 s, the two extreme time points for the data presented here and for earlier transport and conformational change studies: $k_1 = 3.3 \times 10^8\ M^{-1}\ s^{-1}$ (2 ms) and $7.7 \times 10^7\ M^{-1}\ s^{-1}$ (4 s); $k_2 = 33\ s^{-1}$ (2 ms) and $7.7\ s^{-1}$ (4 s).

Note that the rate-constants for conformational changes and charge transport measured earlier with 0.1–1 mM ATP were of the order of $100\ s^{-1}$ [7–10]. Assuming that the second-order rate-constants determined here are applicable to ATP, the pseudofirst-order rate-constants at those concentration of ATP will be $3.3 \times 10^4\ s^{-1}$ (0.1 mM ATP) to $3.3 \times 10^5\ s^{-1}$ (1 mM) at 2 ms and $7.7 \times 10^3\ s^{-1}$ (0.1 mM) and $7.7 \times 10^4\ s^{-1}$ (1 mM) at 4 s. These rate-constants are much faster than the 100–200 s^{-1} seen for conformational changes and charge transport. Thus, the estimated parameters for the stretched exponential indicate that this process is much faster than the conformational changes and charge transfer examined earlier [7–9].

5. Conclusion

Steady-state studies of TNP–ADP and TNP–ATP binding to the enzyme [5,6] have shown that there exist two different population of TNP-nucleotide binding sites on the Na^+/K^+-ATPase, one population (specific) which can bind ATP and the other (nonspecific) which can only bind TNP–ATP. These experiments also indicated that there are a large number of nonspecific binding sites per enzyme molecule.

Equilibrium constants for TNP–ATP and ATP binding to the specific sites were determined. The existence of well-defined equilibrium constants imply that the initial energy (of enzyme + substrate) before binding and the final energy (of the enzyme-substrate complex) are well defined (and time-independent).

Transient state studies of TNP–ATP binding (reported in this paper) are consistent with the existence of specific and nonspecific binding sites. These experiments also indicate that the forward and backward rate-constants are not constant but are distributed around a mean value. This distribution may reflect distributions in the energies of the initial (unbound) state, the final (bound) state, and the transition state. Experiments that specifically probe the kinetics of TNP–ATP binding to the specific binding site suggest that the energy of the transition state for this site is distributed.

Physically, this result may mean that when the specific binding sites are empty or filled, they exist in many different conformations separated from one another by small energy barriers (small as compared with thermal energy). However, these conformations can be distinguished by their transition states, which have different energies. A schematic representation of the energy levels of these states is shown in Fig. 9.

Results reported here indicate that quenching of IAF fluorescence by TNP–ATP is a useful tool for studying the ATP binding site. However, the interpretation of these data is complicated by the presence of nonspecific binding, probably to hydropho-

bic regions within the protein and/or to the lipid bilayer.

Acknowledgements

The authors are indebted to Dr. Sufi Zafar, Motorola, for illuminating discussions on stretched exponentials. Supported by grants from the National Institutes of Health (NS-05430, GM-47550) and the National Science Foundation (DCB-8817355).

References

[1] I.M. Glynn, The Na^+/K^+-transporting adenosine triphosphatase, in: A. Martonosi (Ed.), The Enzymes of Biological Membranes, Vol. 3, Plenum, New York, 1985, pp. 35–114.

[2] J.D. Robinson, M.S. Flashner, The $(Na^+ + K^+)$-activated ATPase. Enzymatic and transport properties, Biochim. Biophys. Acta 549 (1979) 145–179.

[3] S.J.D. Karlish, Characterization of conformational changes in (Na,K)-ATPase labelled with fluorescein at the active site, J. Bioenerg. Biomembr. 12 (1980) 111–136.

[4] E.H. Hellen, P.R. Pratap, Fluorescence quenching of IAF–Na^+/K^+-ATPase via energy transfer to TNP-labelled nucleotide, Proceedings of the VIIIth International Conference on the Na^+/K^+-ATPase, 1996, in press.

[5] E.H. Hellen, P.R. Pratap, Nucleotide binding to IAF-labelled Na^+/K^+-ATPase measured by steady-state fluorescence quenching by TNP–ADP Biophys. Chem. 69 (1997) 107–121.

[6] E.H. Hellen, C.P. Collier, A. Palit, B.C. Yacono, J.M. Fox, P.R. Pratap, TNP–ATP binding to Na^+/K^+-ATPase measured by fluorescence quenching, Biophys. J. 70 (1996) A325.

[7] P.R. Pratap, J.D. Robinson, M.I. Steinberg, The reaction sequence of the Na^+/K^+-ATPase: rapid kinetic measurements distinguish between alternative schemes, Biochim. Biophys. Acta 1069 (1991) 288–298.

[8] P.R. Pratap, J.D. Robinson, Rapid kinetic analyses of the Na^+/K^+-ATPase distinguish between different criteria for conformational change, Biochim. Biophys. Acta 1151 (1993) 89–98.

[9] R. Bühler, W. Stürmer, H.-J. Apell, P. Läuger, Charge translocation by the Na,K-pump: I. Kinetics of local field changes studied by time-resolved fluorescence measurements, J. Membr. Biol. 121 (1991) 141–161.

[10] W. Stürmer, R. Bühler, H.-J. Apell, P. Läuger, Charge translocation by the Na,K-pump: II. Ion binding and release at the extracellular face, J. Membr. Biol. 121 (1991) 163–176.

[11] J.G. Kapakos, M. Steinberg, Fluorescent labelling of (Na+K)-ATPase by 5-iodoacetamidofluorescein, Biochim. Biophys. Acta 693 (1982) 493–496.

[12] J.C. Skou, M. Esmann, The effects of Na^+ and K^+ on the conformational transitions of $(Na^+ + K^+)$-ATPase, Biochim. Biophys. Acta 746 (1983) 101–113.

[13] K. Taniguchi, K. Suzuki, S. Iida, Conformational change accompanying transition of ADP-sensitive phosphoenzyme to potassium-sensitive phosphoenzyme of $(Na^+ + K^+)$-ATPase modified with *N*-[*p*-(2-benzimidazolyl)phenyl]maleimide, J. Biol. Chem. 257 (1982) 10659–10667.

[14] M. Esmann, Determination of rate-constants for nucleotide dissociation from Na,K-ATPase, Biochim. Biophys. Acta 1110 (1992) 20–28.

[15] M. Esmann, Relaxation spectroscopy applied to determination of rate-constants for ligand binding and dissociation, in: E. Bamberg, W. Schoner (Eds.), The Sodium Pump. Structure, Mechanism, Hormonal Control and its Role in Disease, Springer, New York, 1994, pp. 605–608.

[16] P.A.G. Fortes, J.A. Lee, Steady-state levels of phosphorylated intermediates of (Na,K)-ATPase monitored with oligomycin and anthroylouabain, J. Biol. Chem. 259 (1984) 11176–11179.

[17] E.G. Moczydlowski, P.A.G. Fortes, Characterization of 2′3′-*O*-(2,4,6-trinitrocyclohexadienylidene) adenosine-5′-triphosphate as a fluorescent probe of the ATP site of sodium and potassium transport adenosine triphosphate. Determination of nucleotide binding stoichiometry and ion-induces changes in affinity for ATP, J. Biol. Chem. 256 (1981) 2346–2356.

[18] E.G. Moczydlowski, P.A.G. Fortes, Inhibition of sodium and potassium adenosine triphosphatase by 2′3′-*O*-(2,4,6-trinitrocyclohexadienylidene) adenine nucleotides. Implications for the structure and mechanism of the Na:K pump, J. Biol. Chem. 256 (1981) 2357–2366.

[19] P.A.G. Fortes, R. Aguillar, Distances between 5-iodoacetamidofluorescein and the ATP and ouabain sites of (Na,K)-ATPase determined by fluorescence energy transfer, Prog. Clin. Biol. Res. 268A (1988) 197–204.

[20] J.B. Bassingthwaighte, L.S. Liebovitch, B.J. West, Fractal Physiology, Oxford Univ. Press, New York, 1994.

[21] R. Kopelman, Fractal reaction kinetics, Science 241 (1988) 1620–1626.

[22] H.Q. Li, S.H. Chen, H.M. Zhao, Fractal mechanisms for the allosteric effects of proteins and enzymes, Biophys. J. 58 (1990) 1313–1320.

[23] L.S. Liebovitch, T.I. Tóth, Fractal activity in cell membrane ion channels, Ann. NY Acad. Sci. 591 (1990) 375–391.

[24] L.S. Liebovitch, J. Fischbarg, J.P. Koniarek, Ion channel kinetics: a model based on fractal scaling rather than multistate markov processes, Math. Biosci. 84 (1987) 37–68.

[25] A. Ansari, J. Berendzen, S.F. Bowne, H. Fraunfelder, I.E. Iben, T.B. Sauke, E. Shyamsunder, R.D. Young, Protein states and proteinquakes, Proc. Natl. Acad. Sci. 82 (1985) 5000–5004.

[26] P.L. Jørgensen, Purification and characterization of $(Na^+ + K^+)$-ATPase: III. Purification from the outer medulla of mammalian kidney after selective removal of membrane components by SDS, Biochim. Biophys. Acta 356 (1974) 36–52.

[27] P.L. Jørgensen, Isolation of $(Na^+ + K^+)$-ATPase, Meth. Enzymol. 32B (1974) 277–290.

[28] U. Banik, S. Roy, A continuous fluorimetric assay for ATPase activity, Biochem. J. 266 (1990) 611–614.

[29] M. Steinberg, S.J.D. Karlish, Studies on conformational changes in Na,K-ATPase labelled with 5-iodoacetamidofluorescein, J. Biol. Chem. 264 (1989) 2726–2734.

[30] W.C. Hamilton, Statistics in Physical Science, Ronald Press, 1964, 150–157.

[31] A. Plonka, Time-dependent reactivity of species in condensed media, Lecture Notes in Chemistry, Vol. 40, Springer-Verlag, New York, 1986.

[32] T. Ohta, M. Kuroda, M. Yoshii, H. Hayashi, Over-expression of peptide containing the ATP-binding site in Na/K-ATPase α subunit, in: E. Bamberg, W. Schoner (Eds.), The Sodium Pump. Structure, Mechanism, Hormonal Control and its Role in Disease, Springer, New York, 1994, pp. 66–69.

[33] M. Karplus, J.A. McCammon, The internal dynamics of globular proteins, CRC Crit. Rev. Biochem. 9 (1981) 293–349.